

Influence of Sintering Temperature on Pore Structure and Electrical Properties of Technologically Modified MgO-Al₂O₃ Ceramics

Halyna KLYM^{1*}, Ivan HADZAMAN², Oleh SHPOTYUK^{3,4}

¹ Lviv Polytechnic National University, 12 Bandera str., 79013, Lviv, Ukraine

² Drohobych Ivan Franko State Pedagogical University, 24 I. Franko str., 82100, Drohobych, Ukraine

³ Lviv Institute of Materials of Scientific Research Company "Carat", 202 Stryjska str., 79031, Lviv, Ukraine

⁴ Institute of Physics of Jan Dlugosz University, 13/15, al. Armii Krajowej, 42201, Czestochowa, Poland

crossref <http://dx.doi.org/10.5755/j01.ms.21.1.5189>

Received 11 September 2013; accepted 16 February 2014

Technologically modified spinel ceramics are prepared from Al₂O₃ and 4MgCO₃·Mg(OH)₂·5H₂O powders at 1200, 1300 and 1400 °C. The influence of sintering temperature on porous structure and exploitation properties of obtained humidity-sensitive MgO-Al₂O₃ ceramics are studied. It is shown that increase of preparing temperature from 1200 °C to 1400 °C results in transformation of pore size distribution in ceramics from tri- to bi-modal including open macro- and mesopores with the sizes from ten to hundreds nm and nanopores up to a few nm. The studied ceramic elements with electrical resistances $\sim(10^{-2} - 10^3)$ MOhm are high humidity sensitive in the region of 30 % – 95 % with minimal hysteresis in adsorption-desorption cycles. It is established that increasing of humidity sensitivity in ceramics are related to optimum pore size distribution and quantity of pores in the all regions. Prolonged degradation transformation in ceramics at higher temperature and relative humidity results in lose sensitivity.

Keywords: ceramics, porous structure, electrical properties, humidity sensitivity, capillary condensation.

1. INTRODUCTION

Among the large number of porous ceramic materials for humidity sensors [1–3], spinel ceramics are one of the most promising [4–7]. Crystallographic structure of spinel creates opportunity to isotropic grain growth and formation of grain boundaries and open porosity in ceramics [8]. Functional spinel MgO-Al₂O₃ ceramics are more thermal and chemical stable than other types of porous materials with short response times to changes in humidity. Material of active element based on spinel ceramics is promising because it does not require of additional processes of the post-technological optimization [9].

It is well known that exploitation electrical properties of humidity-sensitive elements depend on sorption processes of active materials [10]. Therefore, the actual task appear in relation to preparation of porous materials with controlled microstructure, firstly, with large specific surface area, high open porosity, controlled and optimal pore size distribution [11, 12].

With this aim, the initial powders with different specific surface area and particle size sintered at different temperature are used [11, 13]. Early we studied the effect of initial surface area of powdered materials MgO and Al₂O₃ on the structural properties of the MgAl₂O₄ ceramic sintered at 1100 °C–1400 °C [14]. It was shown, that formation of the main MgAl₂O₄ spinel is substantially intensified with the increase of sintering temperature of ceramics and depended on sintering duration [14]. In addition, sintering temperature influences on formation of pore structure of materials and exploitation properties [15]. The aim of this work is fabrication of modified spinel

ceramics and study of the effect of sintering temperature on pore size distribution and humidity sensitivity of active elements based on MgO-Al₂O₃ ceramics.

2. EXPERIMENTAL

The traditional ceramic technology was used for preparation of spinel MgO-Al₂O₃ ceramics [9, 14]. Equimolar amounts of initial powders (Al₂O₃ with specific surface area of 67 m²/g and 4MgCO₃·Mg(OH)₂·5H₂O with specific surface area of 12.8 m²/g) were mixed in a planetary ball mill for 96 h in an environment with acetone to obtain mixture. The aqueous solution of polyvinyl alcohol was used for obtaining of the molding powder. Bilateral compression was performed in steel molds. After pressing, the samples were sintered in a furnace at 1200, 1300 and 1400 °C for 2 h. Electrical contacts on the planar surface of ceramics were formed by screen printing using Ru-contained paste and Pt contacts. Pre-dried layers of paste were sintered at 850 °C with an exposure of 10 min.

Results obtained with XRD method testify that ceramics sintered at $T_s = 1200\text{ °C} - 1400\text{ °C}$ contain two phases: the main spinel phase and additional MgO phase [9]. The values of XRD parameters of MgO-Al₂O₃ ceramics are shown in Table 1.

Table 1. Phase composition of MgO-Al₂O₃ ceramics

$T_s, \text{ °C}$	Main phase MgAl ₂ O ₄		Additional phase MgO	
	lattice parameter, Å	weight fraction, %	lattice parameter, Å	weight fraction, %
1200	8.0809(2)	93.63(0.78)	4.2124(4)	6.37(0.27)
1300	8.0812(2)	94.12(0.80)	4.2145(4)	5.88(0.30)
1400	8.0808(1)	94.05(0.78)	4.2169(4)	5.95(0.34)

*Corresponding author. Tel.: +380-25827222, fax: +380-2582680.
E-mail address: klymha@yahoo.com (H. Klym)

Structure of grains, grain boundaries and pores were studied using scanning electron microscopy (SEM).

Pore size distribution in MgO-Al₂O₃ ceramics in the region from 2 nm to 1000 nm was studied using Hg-porosimetry (Porosimeter 4000, Carlo Erba Strumentazione) [18].

The humidity sensitivity of ceramics was determined measuring the electrical resistance R on relative humidity RH of environment. The electrical resistance of the studied spinel ceramics was measured in the heat and humidity chamber PR-3E "TABAI" at 20 °C in the region of $RH = 20\% - 99\%$. The electrodes were given on the connecting cables of M-ohmmeter at the fixed frequency of current of 500 Hz (with the aim of avoidance of polarization of adsorbed water molecules) [19]. In addition, for study of stability of ceramic samples in time, the degradation transformation for 240 h at 40 °C and $RH = 95\%$ was carried out.

3. RESULTS AND DISCUSSION

The pore size distributions of technologically modified MgO-Al₂O₃ ceramics obtained at 1200, 1300 and 1400 °C are shown in Fig. 1.

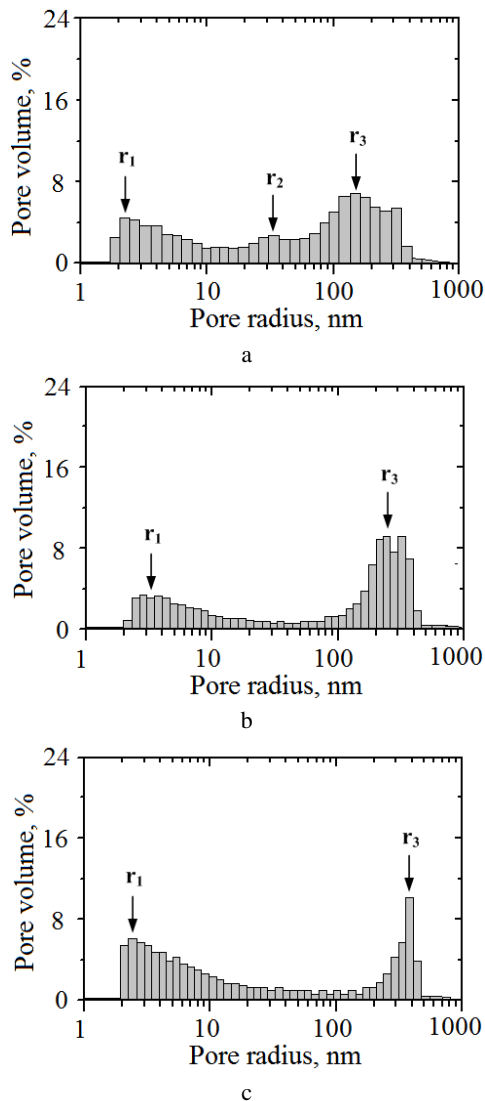


Fig. 1. Pore size distributions of MgO-Al₂O₃ ceramics sintered at 1200 °C (a), 1300 °C (b) and 1400 °C (c)

Such distribution covers the charge-transferring nanopores with r_1 radius depending on sintering conditions, water-exchange inside-delivering or communication mesopores (r_2 radius) and water-exchange outside-delivering macropores (r_3 radius) depending on specific surface area of milled MgO-Al₂O₃ powder. Maximum peak positions (r_1 , r_2 and r_3) and intensities (I_{r1} , I_{r2} and I_{r3}) of pore size distribution for studied ceramics prepared at 1200, 1300 and 1400 °C are shown in Table 1.

Table 1. Peak position of pore size distribution for MgO-Al₂O₃ ceramics sintered at 1200 °C – 1400 °C

T_s , °C	r_1 , nm	I_{r1} , %	r_2 , nm	I_{r2} , %	r_3 , nm	I_{r3} , %
1200	2.3	4.5	35	3.4	160	6.9
1300	2.9	3.2	–	–	270	9.1
1400	2.5	6.0	–	–	380	10.3

It is shown that ceramics sintered at 1200 °C exhibit tri-modal pore size distribution with maximum position of r_1 , r_2 and r_3 near 2.3, 35 and 160 nm, respectively (Table 1 and Fig. 1, a). It is established that large open pores with size near 100 nm–300 nm correspond to open surface pores in ceramics. They provide absorption-desorption process of water from environment. Pores centered near 35 nm are so-called transporting pores providing the effective passing of water into ceramic body.

According to Kelvin equation [16, 17], the open cylindrical nanopores with a radius from smaller 1 nm to 20 nm are required for capillary condensation processes of humidity in ceramics at room temperature in the investigated range of RH (20 %–98 %). Such region includes peak with radius r_1 and partly peak with radius r_2 . Meso- and macropores with radius more that 20 nm (the second and third peak) don't involve in capillary condensation process, but they are needed for effective passing of water into ceramic body.

The obtained results indicate that the sintering temperature influences on the porous structure of ceramics. It is shown, that radius of nanopores r_1 in studied ceramics slightly increases from 2.3 nm for the samples sintered at 1200 °C to 2.9 nm for ceramics obtained at 1300 °C (Fig. 1, a, b). Position of the first peak I_{r1} decreases from 4.5 % to 3.2 % for ceramics sintered at 1200 °C–1300 °C with further growth to 6 % in ceramics obtained at 1400 °C (Fig. 1, d). The position of the second peak with radius r_2 is incidentally pronounced in ceramics sintered at 1200 °C. At that, it is shown that this peak is shifted in direction of the third peak. In ceramics sintered at 1300 °C and 1400 °C, the clear peak position with radius r_2 disappears. But some amount of open mesopores is still remained. So, tri-modal pore size distribution is transformed into bi-modal like in [20]. Obviously, such changes can be attributed to growth of grains during sintering at high temperature with further decreasing of size and amount of pores. Subsequent confluence of pores is accompanied by diminishing of their surface and volume. There is intensive growth of grains and forming of large pores. In result the pore size distribution is shifted to macropores region (Fig. 1, b). Radius r_3 substantially increases from 160 nm to 380 nm with T_s for ceramics obtained from 1200 °C to

1400 °C. The intensity I_{r3} of the third peak narrows increases from 6.9 % to 10.3 % (Table 1 and Fig. 1, b, c).

Evolution of porous structure is supported by the results of SEM investigations (Fig. 2). It is shown, that structure grains and pores in ceramics sintered at 1200 °C is not well formed. Average grain size is near 200 nm. Additional MgO phase is unevenly distributed in the volume of studied ceramics and mostly located near grain boundaries bordering the pores (Fig. 2, a). With the increase of sintering temperature to 1300 °C, the contact area between the grains grows, specific surface area increases, the grains are combined into agglomerates and the amount of open pores increases. Such pores that are initially spherical and the cylindrical shaped are located on the grain boundaries (Fig. 2, b). Average grain size increases to 300 nm – 500 nm. These ceramic samples have better developed porosity (pores transformed in various forms). Along with this, closed porosity is formed due to growth of small pores. These closed pores are not involved in the sorption processes in the studied ceramics.

In ceramics sintered at 1400 °C, the grain structure continues to take shape showing of their intense union. The average size of the grains is near 600 nm – 3000 nm. However, the porous structure is modified mainly due to increasing of closed porosity and reduction of channel transport pores (Fig. 2, c).

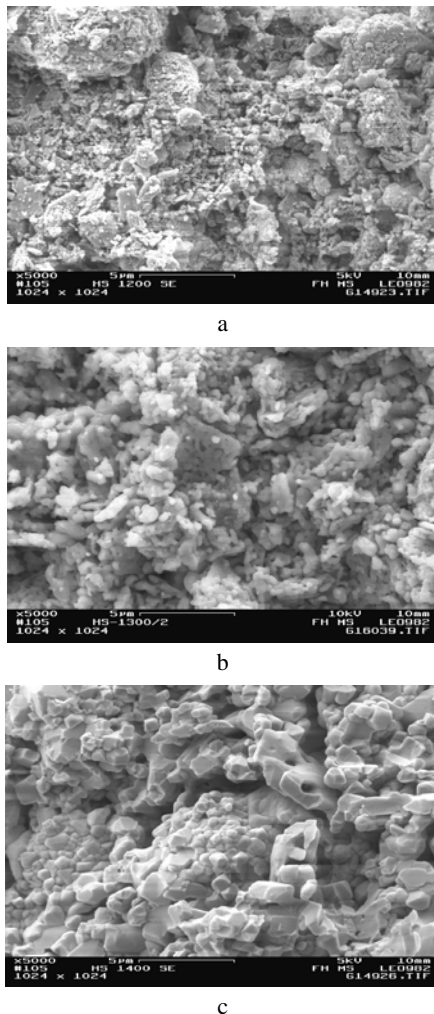


Fig. 2. SEM micrograph of MgO-Al₂O₃ ceramics sintered at 1200 °C (a), 1300 °C (b) and 1400 °C (c)

Changes caused by sintering temperature on pore size distribution were reflected in humidity sensitivity of MgO-Al₂O₃ ceramics. So, ceramics sintered at low temperature (1200 °C) have enough of open pores in all regions. Such behaviour of pore size distribution results in electrical properties of ceramic samples. They have good sensitivity (changes of electrical resistance ~4 orders) between the average values of relative humidity (33 % – 95 %) and minimal hysteresis of dependence in adsorption-desorption cycles (Fig. 3, a). After degradation transformation, this dependence shifts due to saturation of the transport pores.

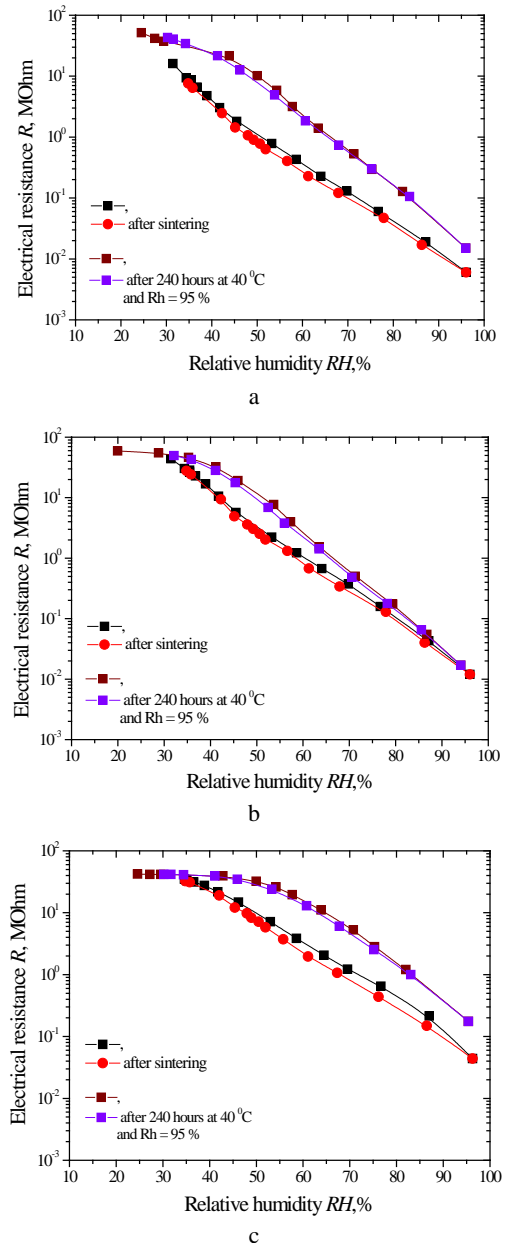


Fig. 3. Exploitation properties of MgO-Al₂O₃ ceramics sintered at 1200 °C (a), 1300 °C (b) and 1400 °C (c)

In spite of a small amount of transporting pores, ceramics sintered at 1300 °C are characterized by linear dependence of electrical resistance R vs. RH in all studied region without significant hysteresis in absorption-desorption cycles (Fig. 3, b). But after degradation tests they loses sensitivity up to 35 %. However, position of the curves before and after degradations do not change substantially.

In contrast to the previous ceramic samples, ceramics sintered at 1400 °C have a small amount of macropores centered near $r_3 = 380$ nm. Humidity-sensitivity of these ceramics are characterized by linearity but with appreciable hysteresis and changes of electrical resistance (Fig. 3, c).

Degradation transformations at 40 °C and $RH = 95$ % result in decreasing of humidity-sensitivity of materials at RH (up to 50 %) just as in ceramics sintered at 1300 °C. Such changes testify to filling of some open nanopores by water and insufficient amount of transporting pores, which does not destroy all water from ceramics.

Thus, humidity sensitivity in ceramics sintered at low 1200 °C and recoverability of electrical characteristic in adsorption-desorption cycles is obviously connected with sufficient of open pores of different size from all pore size distribution region. Increasing of humidity sensitivity and stability of ceramics sintered at 1300 °C result in increase of amount of open water-exchange outside-delivering macropores. They provide efficient sorption processes of water though small amount of communication mesopores.

Bi-modal pore size distribution of ceramics sintered at 1400 °C continues to modify. Capillary condensation processes effective occur due to increasing of amount of transferring nanopores. Hysteresis in absorption-desorption cycles rises over reduction of pores with radius r_3 .

4. CONCLUSIONS

The sintered temperatures allow to refine the most significant changes in porous structure of humidity-sensitive spinel MgO-Al₂O₃ ceramics. Evolution of pore size distribution from tri- to bi-modal in the studied ceramics leads to corresponding changes in their water sorption processes. The increase of humidity sensitivity in ceramics sintered at 1300 °C was related to the optimal pore size distribution. It is shown that in all sintered samples there are pores with radius higher 20 nm, which though do not participate in the processes of capillary condensation, but their presence is needed to support operating in short time in humidity sensitive elements on the change of relative humidity. Degradation transformations at 40 °C and $RH = 95$ % for 240 h result in increasing of humidity-sensitivity of ceramics in all studied region with minimal hysteresis. Such changes testify to the active work of transporting pores after their full saturation of some pores by water.

Acknowledgments

H. I. Klym is kindly grateful for assistance offered by Lviv Polytechnic National University within a grant for young scientists GLP 13/3.

REFERENCES

1. **Chen, Zhi, Lu, Chi.** Humidity Sensors: a Review of Materials and Mechanisms *Sensor Letters* 3 (4) 2005: pp. 274–295.
2. **Kulwicki, B. M.** Humidity Sensors *Journal of the American Ceramic Society* 74 (4) 1991: pp. 697–708. <http://dx.doi.org/10.1111/j.1151-2916.1991.tb06911.x>
3. **Velev, O. D., Kaler, E. W.** Structured Porous Materials via Colloidal Crystal Templating: From Inorganic Oxides to Metals *Advanced Materials* 12 (7) 2000: pp. 531–534.
4. **Vua, D.-H., Wang, K.-Sh., Bac, B. H.** Humidity Control Porous Ceramics Prepared From Waste and Porous Materials *Materials Letters* 65 2011: pp. 940–943.
5. **Cosentino, I. C., Muccillo, E. N. S., Muccillo, R.** The Influence of Fe₂O₃ in the Humidity Sensor Performance of ZrO₂:TiO₂-based Porous Ceramics *Materials Chemistry and Physics* 103 2007: pp. 407–414. <http://dx.doi.org/10.1016/j.matchemphys.2007.02.051>
6. **Cantalini, C., Pelino, M.** Microstructure and Humidity-sensitive Characteristics of a-Fe₂O₃ Ceramic Sensor *Journal of the American Ceramic Society* 75 (3) 1992: pp. 546–551. <http://dx.doi.org/10.1111/j.1151-2916.1992.tb07840.x>
7. **Chou, K.-S., Lee, T.-K., Liu, F.-J.** Sensing Mechanism of a Porous Ceramic as Humidity Sensor *Sensors and Actuators B* 56 1999: pp. 106–111.
8. **Silva, J. B., de Brito, W., Mohallem, N. D. S.** Influence of Heat Treatment on Cobalt Ferrite Ceramic Powders *Materials Science and Engineering B* 112 2004: pp. 182–187.
9. **Klym, H., Ingram, A., Hadzaman, I., Shpotyuk, O., Popov, A., Kostiv, Yu.** Characterization of Microstructural Features of Technologically Modified MgO-Al₂O₃ Ceramics *Journal of Physics: Conference Series* 2014 (in press).
10. **Weaver, P. M., Cain, M. G., Stewart, M., Anson, A., Franks, J., Lipscomb, I. P., McBride, J. P., Zheng, D., Swingler, J.** The Effects of Porosity, Electrode and Barrier Materials on the Conductivity of Piezoelectric Ceramics in High Humidity and Dc Electric Field *Smart Materials and Structures* 21 2012: pp. 045012-9.
11. **Armatas, G. S., Salmas, C. E., Louloudi, M. G., Androutsopoulos, P., Pomonis, P. J.** Relationships Among Pore Size, Connectivity, Dimensionality of Capillary Condensation, and Pore Structure Tortuosity of Functionalized Mesoporous Silica *Langmuir* 19 2003: pp. 3128–3136.
12. **Kashi, M. A., Ramazani, A., Abbasian, H., Khayyatian, A.** Capacitive Humidity Sensors Based on Large Diameter Porous Alumina Prepared by High Current Anodization *Sensors and Actuators A* 174 2012: pp. 69–74.
13. **Zuo, K.-H., Zhang, Y., Zeng, Y.-P., Jiang, D.** Pore-forming Agent Induced Microstructure Evolution of Freeze Casted Hydroxyapatite *Ceramics International* 37 2011: pp. 407–410.
14. **Klym, H., Ingram, A., Shpotyuk, O., Filipecki, J., Hadzaman, I.** Extended Positron-trapping Defects in Insulating MgAl₂O₄ Spinel-type Ceramics *Physica Status Solidi (c)* 4 (3) 2007: pp. 715–718.
15. **Duan, L., Ma, Q.** Effect of Pyrolysis Temperature on the Pore Structure Evolution of Polysiloxane-derived Ceramics *Ceramics International* 38 2012: pp. 2667–2671.
16. **Kohonen, M. M., Christenson, H. K.** Capillary Condensation of Water between Rinsed Mica Surfaces *Langmuir* 16 2000: pp. 7285–7288.
17. **Grosman, A., Ortega, C.** Nature of Capillary Condensation and Evaporation Processes in Ordered Porous Materials *Langmuir* 21 2005: pp. 10515–10521.
18. **Bondarchuk, A., Shpotyuk, O., Glot, A., Klym, H.** Current Saturation in In₂O₃-SrO Ceramics: a Role of Oxidizing Atmosphere *Revista Mexicana de Fisica* 58 2012: pp. 313–316.
19. **Klym, H., Ingram, A., Hadzaman, I., Shpotyuk, O.** Evolution of Porous Structure and Free-volume Entities in Magnesium Aluminate Spinel Ceramics *Ceramics International* 2014 (in press).
20. **Xu, H., Liu, J., Guo, A., Du, H., Hou, Z.** Porous Silica Ceramics with Relatively High Strength and Novel Bi-modal Pore Structure Prepared by a TBA-based Gel-casting Method *Ceramics International* 38 2012: pp. 1725–1729. <http://dx.doi.org/10.1016/j.ceramint.2011.09.013>